Atmos. Chem. Phys. Discuss., 13, 26933–26979, 2013
www.atmos-chem-phys-discuss.net/13/26933/2013/
doi:10.5194/acpd-13-26933-2013

Atmospheric Chemistry and Physics Discussions

Validation of emission inventories by measurements of ambient volatile organic compounds in Beijing, China

M. Wang[1], M. Shao[1], W. Chen[1], B. Yuan[1,*], S. Lu[1], Q. Zhang[2], L. Zeng[1], and Q. Wang[1,3]

[1]State Joint Key Laboratory of Environmental Simulation and Pollution Control, College of Environmental Sciences and Engineering, Peking University, Beijing, China
[2]Ministry of Education Key Laboratory for Earth System Modeling, Center for Earth System Science, Tsinghua University, Beijing, China
[3]Beijing Municipal Environmental Monitoring Center, Beijing, China
[*]now at: NOAA Earth System Research Laboratory and Cooperative Institute for Research in Environmental Sciences, University of Colorado, Boulder, CO, USA

Received: 21 September 2013 – Accepted: 1 October 2013 – Published: 16 October 2013

Correspondence to: M. Shao (mshao@pku.edu.cn) and
M. Wang (wangmingmelon@163.com)

Published by Copernicus Publications on behalf of the European Geosciences Union.

Abstract

Understanding the sources of volatile organic compounds (VOCs) is essential for ground-level ozone and secondary organic aerosols (SOA) abatement measures. We made measurements at 28 sites and online observations at an urban site in Beijing from July 2009 to January 2012. From these we determined the spatial and temporal distributions of VOCs, estimated their annual emission strengths based on their emission ratios relative to CO, and quantified the relative contributions of various sources using the chemical mass balance (CMB) model. The results from ambient measurements were compared with existing emission inventories to evaluate the spatial distribution, species-specific emissions, and source structure of VOCs. The measured VOC distributions revealed a hotspot in the southern suburban area of Beijing, whereas current emission inventories suggested that VOC emissions were concentrated in downtown areas. Compared with results derived from ambient measurements, the annual inventoried emissions of oxygenated VOC (OVOC) species and C2–C4 alkanes might be underestimated, while the emissions of styrene and 1,3-butadiene might be overestimated by current inventories. Source apportionment using the CMB model identified vehicular exhaust as the most important VOC source, contributing 46 %, in good agreement with the 40–51 % assumed by emission inventories. However, the relative contribution of solvent and paint usage obtained from the CMB model was only 5 %, significantly lower than the values reported by emission inventories (14–32 %). Meanwhile, the relative contribution of industrial processes calculated using the CMB model was 17 %, slightly higher than that in emission inventories. These results suggested that VOCs emission strengths in southern suburban area of Beijing, annual emissions of alkenes and OVOCs, and the contributions of solvent and paint usage and industrial processes in current inventories, all require significant revision.

1 Introduction

Volatile organic compounds (VOCs) play important roles in atmospheric chemistry because they can be photochemically oxidized to form ground-level ozone (O_3) and secondary organic aerosols (SOA) (Seinfeld and Pandis, 2006). In Beijing and its surrounding areas, air pollution complex characterized by concurrent high ground-level $O_3$and fine particle ($PM_{2.5}$) concentrations has become a severe problem (Shao et al., 2009). Obtaining accurate knowledge on VOC emissions and sources is essential to understanding their roles in ozone and SOA formation, and in establishing effective control measures to reduce the ambient concentrations of these secondary pollutants (Liu et al., 2013).

VOCs can be directly emitted to the atmosphere from both natural and anthropogenic processes, and they may also be formed as products of the photochemical oxidation of other VOC species. On a global scale, natural emissions are the most important VOCs sources, whereas anthropogenic emissions are dominant in most urban areas (Atkinson and Arey, 2003). Emission inventories can provide information on emission magnitudes, the spatial and temporal distribution of emissions, and the source characteristics of individual VOC species. The construction of emissions datasets is achieved using a "bottom-up" approach, summing the products of activity data and emission factors for known individual sources. However, the establishment of emission inventories for non-methane VOCs (NMVOCs) is not only time- and resource-consuming, but also plagued by large and inherent uncertainties due to the inaccurate and incomplete local knowledge of NMVOCs emissions (e.g., source profiles, emission factors, and source activities). Several studies have built emission inventories for anthropogenic VOCs in Beijing (Klimont et al., 2002; Streets et al., 2003; Ohara et al., 2007; Bo et al., 2008; Wei et al., 2008; Zhang et al., 2009; Su et al., 2011; Zhao et al., 2012); however, their results have been inconsistent with each another (Fig. S1). Zhang et al. (2009) reported that the annual emission of anthropogenic NMVOCs from Beijing in 2006 was 496 Gg, higher than the year 2005 emissions of 333 Gg reported by Wei et al. (2008) and 301 Gg

reported by Bo et al. (2008). In addition, the spatial distribution of NMVOC emission strengths in Beijing reported by Zhang et al. (2009) illustrated that the largest emission sources were in southern areas, whereas Zhao et al. (2012) reported NMVOC emission sources were mainly concentrated in the downtown area. Although each of these inventories indicates that vehicular emission is the most important NMVOC source in Beijing, the contributions from industrial processes and solvent and paint utilization showed significant disagreements (see Table 1). Zhang et al. (2009) reported that industrial processes contributed 41 % of NMVOCs emissions in Beijing, whereas Zhao et al. (2012) estimated that industrial processes contributed only 3 %. The contribution of solvent and paint utilization estimated by Wei et al. (2008) was 32 %, significantly higher than the value of 14 % reported by Bo et al. (2008). Comparisons among different emission inventories reveal uncertainty regarding NMVOCs sources in terms of annual emissions, spatial distribution, and source structure. However, this comparison could not quantify the uncertainty, nor could it evaluate the accuracy of NMVOC emission inventories. An alternative method of proceeding is to use measurement data to evaluate and improve the degree of consistency between measurements and emission inventories, a technique that is often termed a "receptor-oriented" or "top-down" method. Since the measured concentration of NMVOCs is actually the result of emissions after physical (transport/mixing/deposition) and chemical transformations, various approaches need to be employed to build relationships between measurements and emission data.

Previous studies applied tracer ratio methods to estimate the anthropogenic emissions of individual NMVOC species (Hsu et al., 2010; Shao et al., 2011; Yao et al., 2012). In this method, carbon monoxide (CO) is usually chosen as the reference tracer because the measured mixing ratios of CO showed significant correlations with the measured levels of most anthropogenic VOCs (Baker et al., 2008; von Schneidemesser et al., 2010). Another reason for using CO as a reference tracer is that CO emissions inventories in China have recently been validated using measured atmospheric data (Tang et al., 2013; Heald et al., 2003) and that CO emissions are relatively well un-

derstood. However, the measured ratios of VOCs levels relative to CO (VOC/CO) will change with photochemical processing because CO is less photochemically reactive than most VOC species and further some carbonyl compounds may be photochemically produced. De Gouw et al. (2005) and Warneke et al. (2007) examined the oxidation of VOC species by OH radicals and developed parameterization equations to describe the photochemical evolution of VOC/CO ratios and to calculate the emission ratios of anthropogenic VOCs relative to CO. The anthropogenic emissions of VOC species were then calculated based on the derived VOC emission ratios and the known emission rate of a reference compound.

Three-dimensional air quality models are increasingly being used to evaluate and validate VOC emission inventories through comparing simulated and observed concentrations. Coll et al. (2010) and Chen et al. (2010) compared VOC surface observations in Marseille (France) and Taiwan with regional-scale model simulations and found large differences between measurements and emission model outputs, indicating that many VOC emissions from inventories require correction. Fu et al. (2007) and Liu et al. (2012a) applied inverse modeling techniques based on chemical transport models to constrain formaldehyde (HCHO) and glyoxal (CHOCHO) precursor emissions in China based on satellite observations, respectively. In the study by Fu et al. (2007), the total emissions of HCHO precursors constrained by HCHO columns were higher than the total emissions from bottom-up inventories. In addition, Liu et al. (2012a) found that the discrepancy between modeled CHOCHO and observed CHOCHO columns was likely caused by the underestimation of aromatic emissions in current inventories.

Receptor models based on ambient and source measurements can be used to evaluate the accuracy of different source contributions to VOCs in inventories (Fujita et al., 1995; Niedojadlo et al., 2007). Recently, VOC source apportionment has been intensively studied in Beijing using receptor models (Wang et al., 2010; Song et al., 2007). These studies showed motor vehicles (in particular gasoline-powered vehicles) to be the main source of ambient non-methane hydrocarbons (NMHCs), with relative contributions of 52–69 %. However, the vehicular contribution to NMVOCs in the most recent

emission inventory was only 41 %, compared with a solvent utilization estimate of more than 30 % (Su et al., 2011). Besides the inherent uncertainties in both VOC emission inventories and receptor model results, another possible reason for this discrepancy is that the previous receptor models were based on ambient data from limited sites over short time periods, whereas emission inventories have generally been established on an annual basis for an entire city. Therefore, in order to compare VOC source structures between these two methods, more ambient city-scale measurements, over annual intervals, are required.

In this study, we first present the temporal and spatial distributions of VOCs in Beijing based on a VOCs grid study and other online measurements conducted in Beijing from July 2009 to January 2012. Then, the emission ratios of individual VOC species to CO are determined in order to calculate the annual emissions of individual VOC species. Finally, the relative contributions of different sources to NMHCs are quantified using the chemical mass balance (CMB) receptor model. These results from ambient measurements are compared with existing emission inventories to evaluate the accuracy of those inventories from the perspectives of spatial distribution, emissions of individual VOC species, and the relative contributions from different sources.

2 Methods

2.1 VOC sampling and analysis

2.1.1 Online measurements of VOCs

Online measurements of VOCs were conducted during summer (30 July to 20 September 2011) and winter (29 December 2011 to 18 January 2012) from the top of a six-story building on the Peking University campus in Beijing (the PKU site, 40.00° N, 116.31° E). This site, which is located 10 km northwest of Beijing city center and about

200 m north of the fourth ring road, represents a typical urban environment in Beijing (Liu et al., 2009; Wang et al., 2010).

Ambient C2–C12 non-methane hydrocarbons (NMHCs), C3–C6 carbonyl compounds, C1–C2 halocarbons, and C1–C4 alkyl nitrates were measured using an online automated gas chromatography (GC) system, coupled with a low-temperature, cryogen-free pre-concentration device. Detailed analytical methods, quality control, and quality assurance (QA/QC) procedures for this system have been described elsewhere (Wang et al., 2013; Yuan et al., 2012). Formaldehyde and acetaldehyde were measured using a commercial high-sensitivity (HS) proton transfer reaction mass spectrometer (PTR-MS) (Ionicon Analytik, Innsbruck, Austria). The PTR-MS set-up and QC/QA details have been reported by Yuan et al. (2012).

Ambient levels of CO, O_3 and NO_x were measured using a commercial infrared filter correlation analyzer (Model 48i, TEI, USA), a UV photometric analyzer (Model 49i, TEI) and a chemiluminescence trace-level analyzer (Model 42i-TL, TEI), respectively.

2.1.2 Offline VOC measurements at 27 sites in Beijing

Whole air samples were collected at 27 sites in Beijing from July 2009 to January 2011 (see the blue triangles in Fig. 1). These sites were grouped into five categories based on their geographic locations, prevailing monsoon wind directions, and proximity to major roadways (Table S1). *Urban*,*Suburban_South*,*Suburban_North*, and *Rural* categories included sites located in the central downtown, southern suburb, northern suburb, and western rural areas of Beijing, respectively. Most sites were placed ∼ 3–20 m a.g.l. in well-ventilated areas, such as parks and schools, to avoid the potential influences of local sources. The *Roadside* sites were near roadways to investigate the influences of traffic-related sources. The sites, along with environmental automatic air quality monitoring stations, were given priority.

Ambient air was instantaneously sampled using 3.2 L fused silica stainless steel canisters (Entech Instruments, Simi Valley, CA, USA) that had been pre-cleaned with high-purity nitrogen and evacuated with an Entech 3100 automated canister cleaner (Entech

Instruments, USA). Most sampling campaigns were conducted on days characterized by low wind speed, high relative humidity, and poor visibility. After sampling, these canisters were returned to the laboratory in Peking University within one week to analyze the target compounds using a three-stage cryofocusing pre-concentration system (Entech 7100, Entech Instruments) and analyzed with a GC (HP-7890A, Agilent Technologies, Santa Clara, CA, USA). The analytical methods and QC/QA procedures for this system have been described in detail by Liu et al. (2008b) and Wang et al. (2010). The 55-NMHCs standard gas (Spectra Gases, Inc.) was used to calibrate the C2–C12 NMHCs. The MDLs of C2–C12 NMHCs were in the ranges of 0.003–0.012 ppbv.

Carbonyl compounds were measured at 27 sites in Beijing by in situ derivatization sampling using dinitrophenylhydrazine (DNPH)-coated C18 cartridges (Waters and Associates, Milford, MA, USA) during July–September 2010 and January 2011. Ambient air was collected at a flow rate of 100 L min^{-1} through a KI ozone scrubber over two 3 h sampling periods on each sampling day (i.e., 09:00–12:00 LT and 13:00–16:00 LT). The cartridges were then eluted with 5 mL acetonitrile in the laboratory and analyzed using high-performance liquid chromatography (HPLC), following the TO-11A procedure recommended by the US Environmental Protection Agency (EPA, Washington, DC, USA).

The CO levels in ambient air were quantified using an improved GC-FID system with a home-built low-pressure injector. The air in the canisters was first compressed to 1 atm and then each 10 mL aliquot was injected into the gas chromatograph system (HP-6890A, Hewlett Packard, USA) using two molecular-sieve-packed columns in series to separate the CO and methane. The first column was filled with 5 Å particles and was 1.8 m long, while the second was packed with TDX01 and was 2 m long. During this analysis, the GC was operated isothermally at a column temperature of 105 °C. Column elutes were allowed to pass through the methane reformer using nickel as a catalyst, operated at 400 °C, to convert CO into methane, which was subsequently detected by the FID. Details of this system are provided in Wu et al. (2010).

Ambient O_3, NO, and NO_2 data were obtained from automatic air monitoring stations operated by the Beijing Municipal Environment Monitoring Center.

2.2 Receptor model

The chemical mass balance model (CMB version 8.2), which was developed by the US EPA, was used to conduct VOC source apportionment (Wang et al., 2010). The contribution from each source was estimated based on the source profiles and chemical speciation of ambient samples using the following mass balance equation:

$$c_i = \sum_{j=1}^{J} \alpha_{ij} S_j \quad (i = 1, 2, \ldots, I) \tag{1}$$

where c_i is the ambient mass concentration of compound i measured at receptor sites, α_{ij} is the percentage of compound i in an emission source j, S_j is the contribution of source j to the ambient sample, and I and J are the number of compounds and sources, respectively. Therefore, ambient VOC concentrations and source profiles are the two CMB model inputs. The source profiles used in this work were measured in China (Liu et al., 2008a).

The "fitting" species were selected based on the following criteria: (1) they are major constituents of ambient samples and source emissions, and (2) their atmospheric lifetime is longer than that of toluene (i.e., more reactive VOC species such as alkenes and C8–C9 aromatics were not included). Consequently, 25 VOC species were selected as fitting species, including C2–C9 alkanes, acetylene, benzene, toluene, and isoprene. It should be noted that isoprene was included as a fitting species even though it is more reactive than toluene, because it is the only compound that was present in the biogenic source profile.

3 Results and discussion

3.1 Spatial distribution of VOC mixing ratios

The gridded measurements in Beijing were conducted during periods with wind speeds $< 1.5\,m\,s^{-1}$, and therefore the spatial distribution of measured VOC mixing ratios could to some extent reflect the spatial patterns of VOC emission strengths. Based on the annual average mixing ratios of trace gases at each site, the universal Kriging method was applied to predict contour plots of NMHCs (i.e., the summed mixing ratios of measured NMHC species), carbonyls (i.e., the summed mixing ratios of measured carbonyl compounds), CO, and NO_x in Beijing (Fig. 1a–d).

The measured NMHCs, carbonyls, CO, and NO_x levels displayed similar spatial patterns, with the highest concentrations in central (urban) and southern areas of Beijing. However, the emission inventories reported by Tang et al. (2010) and Wang et al. (2009) suggested that VOC and NO_x emissions in Beijing were concentrated in downtown areas, with emission strengths that exceeded those in suburban areas by factors of $\sim$ 5–20. It should be noted that the NMVOC emission inventories reported by Wang et al. (2009) and Tang et al. (2010) were established based on activity data collected in 2000 and 2006, respectively, whereas our measurements were conducted from 2009 to 2012. During the last two decades, the spatial distribution of industry in Beijing has been evolving. High pollution industries have gradually moved out of the urban center of Beijing; and meanwhile, industrial clusters have been developed in suburban areas (Beijing Municipal Commission of Economy and Information Technology, http://www.bjeit.gov.cn/). The Beijing Economic-Technological Development Area (BDA) – located in the southern area of Beijing (see BOS1 in Fig. 1), one of the fast-growing industrial zones contributed 16.3 % of Beijing's total industrial production in 2010 (Beijing Municipal Bureau of Statistics, http://www.bjstats.gov.cn/). In parallel with rapid economic development, southern suburban areas of Beijing have become more urbanized during recent years. As a result of these spatial changes, hotspots of anthropogenic pollutant emissions have potentially extended into southern suburban areas

of Beijing. The differences between measurements and emission inventory records of VOC spatial distribution indicated that current emission inventories might not accurately reflect the spatial distribution of anthropogenic VOCs emissions in Beijing. Therefore, an updated VOC emission inventory for Beijing with a high spatial resolution is urgently needed for to gain a better understanding of the regional pollution from O_3 and SOA based on chemical transport models.

3.2 Temporal variations in VOC species

The chemical composition of ambient VOCs can be affected by their emission and their photochemical removal or formation. In order to investigate seasonal variations in VOC sources and photochemistry, the monthly variations in some representative VOC ratios were examined at urban sites in Beijing. Figure 2a–c shows seasonal variations in the ratios of *i*-pentane to acetylene, toluene to ethene, and isoprene to 1,3-butadiene, respectively. These three hydrocarbon pairs have similar reactivity, but different sources. Vehicular exhaust was found to be the dominant source of acetylene, ethene, and 1,3-butadiene in Beijing (Wang et al., 2010), while *i*-pentane, toluene, and isoprene were also influenced by gasoline evaporation (Liu et al., 2008a), solvent and paint utilization (Yuan et al., 2010), and biogenic emissions (Fuentes et al., 1996), respectively. The ratios of both *i*-pentane to acetylene and toluene to ethene, exhibited higher values in summer than in winter (Fig. 2a and b), because the high ambient temperatures in summer can increase the evaporation rate of VOCs from gasoline and paint. Isoprene and 1,3-butadiene levels measured from November to March showed a significant correlation (r = 0.75) with an average ratio of isoprene/1,3-butadiene of 0.29 ppbv ppbv^{-1}, close to the value from a tunnel study of 0.34 ppbv ppbv^{-1} in Beijing (Wang et al., 2010), indicating that vehicular exhaust was the dominant source of wintertime isoprene. However, measured ratios of isoprene/1,3-butadiene from May to September were 16–43 ppbv ppbv^{-1}, higher than wintertime ratios by factors of > 50 (Fig. 2c), indicating that biogenic emissions dominate summertime isoprene. Figure 2d shows the monthly variations in ethene and acetylene. Although these two species are both

mainly from combustion sources (Wang et al., 2010), they have different atmospheric lifetimes (Atkinson et al., 2006), and therefore the variation in their ratios may reflect the photochemical degree of sampled air masses. The ratios of ethene/acetylene from June to October were 0.6–0.8 ppbv ppbv^{-1}, significantly lower than the ratios from November to March (1.0–1.5 ppbv ppbv^{-1}), indicating the influence of photochemistry on the chemical composition of VOCs during the summer.

To further investigate the effect of photochemistry on the chemical composition of VOCs during the summer, the average diurnal profiles for the ratios of benzene, *trans*-2-pentene, *i*-$BuONO_2$, and acetaldehyde to acetylene measured at the PKU site were examined (Fig. 3). The atmospheric lifetime for benzene (k_{OH} = 1.2 × 10^{-12} cm^3 molecule^{-1} s^{-1}) is similar with that for acetylene (k_{OH} = 1.0 × 10^{-12} cm^3 molecule^{-1} s^{-1}), and therefore the ratios of benzene/acetylene exhibited relatively flat diurnal variations (Fig. 3a). Conversely, the measured ratios of *trans*-2-pentene/acetylene exhibited a significant decrease during the morning (~ 05:00–09:00 LT), since *trans*-2-pentene was photochemically removed more rapidly than acetylene (k_{OH} for *trans*-2-pentene is 6.7 × 10^{-11} cm^3 molecule^{-1} s^{-1}). In contrast to the average diurnal profile for*trans*-2-pentene/acetylene, the measured ratios of *i*-butyl nitrate (*i*-$BuONO_2$) and acetaldehyde to acetylene both exhibited a significant increase from 07:00 LT until they reached maximum values in the afternoon (~ 13:00 to 16:00 LT), indicating the strong photochemical production of these species during summer daytime hours. These findings suggest that photochemistry is another important factor to influence VOC ratios in atmosphere besides the difference of VOC chemical composition from various sources; therefore, to derive VOC emission characteristics from measurements, the photochemical removal or production of VOC must be considered and excluded.

3.3 Annual anthropogenic emissions of VOC species

The anthropogenic emissions of VOC species can be estimated by their emission ratios to a reference compound and the known emissions of the reference compound. This

approach is based on the assumption that the emissions of target VOC species and the reference compound are synchronous, and their emission ratios are only affected by photochemical processing. Two important steps of this method include (1) the selection of a suitable reference compound and (2) the derivation of emission ratios for individual VOC species from measurement data.

3.3.1 Selection of a reference compound

The selection of the reference compound for anthropogenic VOC species should consider the following criteria: (1) the reference compound should have similar sources to anthropogenic VOC, and (2) the uncertainty of its emissions should be lower than that of VOC emissions. In this study, we selected CO as the reference compound, for the following reasons. For one, previous studies on VOC sources suggested that vehicular emissions were the dominant source in Beijing, with a relative contribution of > 40 % (Wang et al., 2010; Zhang et al., 2009; Song et al., 2007). Emissions of CO, a product of the incomplete combustion of fuels, are also dominated by vehicular emission in urban areas (Baker et al., 2008; Parrish, 2006; von Schneidemesser et al., 2010). Secondly, the CO emissions of Beijing were recently validated based on measured data (Tang et al., 2013), and thus the uncertainty of the CO emission inventory was much lower than that of VOC emissions.

To further check the rationality of selecting CO as the reference compound, the correlations between mixing ratios of individual VOC species and CO levels were analyzed. Considering all ambient samples collected in Beijing as an entire data set, all anthropogenic VOC species showed significant correlations with CO at the 0.01 level (two-tailed). Acetylene, ethane, propane, and benzene had the strongest correlation with CO ($r > 0.8$). The weakest correlations with CO were found for C8–C9 aromatics ($r = 0.41$–0.65), C4–C5 alkenes ($r = 0.47$–0.73), and carbonyls ($r = 0.48$–0.67). One possible explanation for the relatively poor correlations of these species with CO is that their ratios to CO are influenced by photochemical processing. Figure 4a and b shows the scatter plots of 1-butene and formaldehyde vs. CO, respectively, measured

at the PKU site in summer of 2011. The measured ratios of 1-butene/CO decreased, but formaldehyde/CO increased with rising O_3 levels. This is because reactive aromatics and alkenes were photochemically removed more rapidly than CO, while carbonyls were produced by photochemical processing.

3.3.2 Derivation of emission ratios for individual VOC species

The emission ratios of VOC to CO can be determined by two approaches from measurement data. The first method is to derive the slope of VOC concentrations to CO using a linear, two-sided least-square fit to the observations (orthogonal distance regression [ODR] linear regression method), with the y-intercept allowed to vary. To minimize the effects of photochemical processing, online measurement data obtained from 03:00–07:00 LT at the PKU site, and observation data at 09:00 LT from regional measurements, were used to calculate VOC emission ratios using the ODR linear regression method. The other method is based on the photochemical evolution of the ratio of VOC to CO as air mass ages (the $[OH]\Delta t$ method), a method first introduced by de Gouw et al. (2005) and Warneke et al. (2007). In this method, the photochemical removal of VOC species is assumed to be dominated by a reaction with the OH radical. The photochemical evolution of measured ratios of hydrocarbon (HC) with CO can be described by the following equation:

$$\frac{[HC]}{[OH]} = ER_{HC} \times \exp\left(-\left(k_{HC} - k_{CO}\right)[OH]\Delta t\right) \quad (2)$$

where [HC]/[CO] is the measured ratio of particular hydrocarbon HC to CO, ER_{HC} is the emission ratio of HC to CO, and k_{HC} and k_{CO} are the rate constants for the oxidation of HC and CO by the OH radical, respectively. The OH exposure ($[OH]\Delta t$) is defined as the integral of OH abundance extending from the time of emission (t_E) to the time of measurement (t_M). The derivation of oxygenated VOC (OVOC) emission ratios from ambient measurements is more complicated due to their photochemical production by

hydrocarbon oxidation, and by the possible influence of biogenic sources and background concentrations. De Gouw et al. (2005) developed a multivariable regression method to calculate OVOC emission ratios as follows:

$$\begin{aligned}[\mathrm{OVOC}] = & \mathrm{ER}_{\mathrm{OVOC}} \times [\mathrm{CO}] \times \exp\left(-\left(k_{\mathrm{OVOC}} - k_{\mathrm{CO}}\right)[\mathrm{OH}]\Delta t\right) \\ & + \mathrm{ER}_{\mathrm{precursor}} \times [\mathrm{CO}] \times \frac{k_{\mathrm{precursor}}}{k_{\mathrm{OVOC}} - k_{\mathrm{precursor}}} \\ & \times \frac{\exp\left(-k_{\mathrm{precursor}}[\mathrm{OH}]\Delta t\right) - \exp\left(-k_{\mathrm{OVOC}}[\mathrm{OH}]\Delta t\right)}{\exp\left(k_{\mathrm{CO}}[\mathrm{OH}]\Delta t\right)} \\ & + ([\mathrm{biogenic}] + [\mathrm{background}]) \end{aligned} \quad (3)$$

where $\mathrm{ER}_{\mathrm{OVOC}}$ and $\mathrm{ER}_{\mathrm{precursor}}$ are the emission ratios of OVOC and their anthropogenic precursors, respectively. In Eq. (3), the first and second terms represent the photochemical removal of OVOC species from primary emissions and the secondary production by anthropogenic precursor oxidation, respectively. The [biogenic] term represents OVOC from biogenic emissions or produced by biogenic NMHC oxidation. The [background] term means the background mixing ratios of OVOC.

In the latter method, determining the extent of photochemical aging of air masses (i.e., OH exposure) is the basis of deriving VOC emission ratios. The OH exposure can be calculated based on the measured ratio of two hydrocarbons with similar sources but different lifetimes, using the following equation:

$$[\mathrm{OH}]\Delta t = \frac{1}{k_{\mathrm{HC}_1} - k_{\mathrm{HC}_2}} \times \left(\ln\left(\frac{[\mathrm{HC}_1]}{[\mathrm{HC}_2]}\right)_{t=0} - \ln\left(\frac{[\mathrm{HC}_1]}{[\mathrm{HC}_2]}\right)\right) \quad (4)$$

where $[\mathrm{HC}_1]/[\mathrm{HC}_2]$ is the measured ratio of HC_1 to HC_2. $([\mathrm{HC}_1]/[\mathrm{HC}_2])t = 0$ is the emission ratio of HC_1 to HC_2. The value of $([\mathrm{HC}_1]/[\mathrm{HC}_2])t = 0$ is estimated at the highest ratio of $\mathrm{HC}_1/\mathrm{HC}_2$ during the night from its diurnal variation profile (see the dashed line in Fig. 5a).

Another method to determine OH exposure is based on the sequential reaction model of alkyl nitrates (RONO_2) developed by Bertman et al. (1995):

$$[\mathrm{OH}]\Delta t = \frac{[\mathrm{OH}]}{k_{\mathrm{A}} - k_{\mathrm{B}}} \times \left(\ln\left(\frac{[\mathrm{RONO}_2]}{[\mathrm{RH}]} - \frac{\beta k_{\mathrm{A}}}{k_{\mathrm{B}} - k_{\mathrm{A}}}\right) - \ln\left(\left(\frac{[\mathrm{RONO}_2]_0}{[\mathrm{RH}]_0}\right) - \frac{\beta k_{\mathrm{A}}}{k_{\mathrm{B}} - k_{\mathrm{A}}}\right)\right) \quad (5)$$

where $k_{\mathrm{A}} = k_{\mathrm{RH}}[\mathrm{OH}]$ and $k_{\mathrm{B}} = k_{\mathrm{RONO}_2}[\mathrm{OH}] + J_{\mathrm{RONO}_2}$ are the pseudo-first-order rate constants for the production and destruction of RONO_2, respectively. k_{RH} and k_{RONO_2} are the rate constants of parent alkane RH and RONO_2 reactions with the OH radical, respectively. J_{RONO_2} is the photolysis rate of RONO_2, the values of which were taken from Bertman et al. (1995). [OH] is the average abundance of the ambient OH radical from emission time to measurement time, which was assumed to be 5×10^6 and 1×10^6 molecule cm^{-3} in summer and winter, respectively, according to measured and modeled OH abundance in Beijing (Takegawa et al., 2009; Liu et al., 2012b; Lu et al., 2013). The factor β is the fraction ratio of RONO_2 production from the reaction of RH with the OH radical, the values of which were taken from Kwok and Atkinson (1995). The $[\mathrm{RONO}_2]_0/[\mathrm{RH}]_0$ is the initial ratio of RONO_2 with CO at emission time before undergoing photochemical processing, the values of which were estimated to be lowest during the nighttime based on its diurnal variation profile (see the dashed line in Fig. 5b). The values of the VOC rate constants with OH radicals were taken from Atkinson et al. (2006). In this study, the ratios of *o*-xylene to ethylbenzene (X/E) and *i*-BuONO_2 to *n*-butane were selected to estimate OH exposure ($[\mathrm{OH}]\Delta t_{\mathrm{X/E}}$ and $[\mathrm{OH}]\Delta t_{\mathrm{AN}}$) using Eqs. (4) and (5), respectively.

Figure 6a and b compares the summertime emission ratios for individual VOC species calculated using the $[\mathrm{OH}]\Delta t$ method and the ODR linear regression method at the PKU site. The VOC emission ratios calculated based on $[\mathrm{OH}]\Delta t_{\mathrm{X/E}}$ and $[\mathrm{OH}]\Delta t_{\mathrm{AN}}$ correlated well ($r = 0.997$), with a linear regression slope of 1.08. The VOC emission ratios from the ODR linear regression method were generally within a factor of two of values from the $[\mathrm{OH}]\Delta t$ method. However, the emission ratios (ERs) for some OVOC species (e.g., propanal, methyl ethyl ketone [MEK]) were overestimated by the linear

regression method, whereas the ERs for some reactive alkenes (e.g., propene, *trans*-2-butene, and 1,3-butadiene) were underestimated. This is possibly due to the influence of OVOC photochemical production and the photochemical removal of alkenes. In the following sections, we use the emission ratios calculated using the [OH]Δt method to investigate the seasonal variation in VOCs and to calculate their annual emissions in Beijing.

3.3.3 Temporal variations in VOC emission ratios at the PKU site

Figure 7a compares the emission ratios of VOC species to CO in the summer and winter. The emission ratios of most VOC species were lower in the winter than in the summer, with the exception of acetylene, ethene, propene, 1,3-butadiene, benzene, ethane, and formaldehyde. This discrepancy between summertime and wintertime emission ratios of most VOC species is possibly due to the seasonal variation in VOC sources in Beijing. During the winter, more fuels (e.g., coal and natural gas) are burned for heating, and thus combustion processes make greater contributions to VOC emissions. However, VOC emission rates from evaporation processes (e.g., gasoline, liquefied petroleum gas, and solvent) are greater in the summer owing to high ambient temperatures. As noted above, CO is mainly emitted from incomplete combustion processes, and therefore the emission ratios of VOC species from non-combustion sources (e.g., propane, toluene, and acetone) are lower in winter. However, the wintertime emission ratios of these VOC species (e.g., acetylene, ethene, benzene, and formaldehyde) are mainly related to combustion processes, and were close to those values found in the summer. Further discussions on the seasonal variations in VOC sources are presented in Sect. 3.4.1.

Figure 7b–d compares the summertime emission ratios of individual VOC species with those derived from online VOC measurements during 2010 (Yuan et al., 2012), 2008 (Wang et al., 2010), and 2005 (Liu et al., 2009), and during 2011 at the PKU site. The VOC emission ratios in 2010 and 2008 correlated well with the values from 2011 (r = 0.99 for 2010, r = 0.96 for 2008), with linear regression slopes of 0.91 ± 0.02

and 1.15 ± 0.05, respectively. These results suggest a similarity between VOC sources from 2008 to 2011. The NMHC emission ratios in 2005 agreed well with the values from 2011 within a factor of two (r = 0.83, slope = 0.70). However, the emission ratios of methanol, acetone, and MEK in 2011 were larger than those in 2005 by a factor of approximately three.

3.3.4 Comparison with VOC emission ratios obtained in other cities

Figure 8a–h compares VOC emission ratios at the PKU site with other measurement datasets. The VOC emission ratios at the PKU site correlated well with those from the three other datasets in China (r = 0.94–0.99), including regional measurements in Beijing, measurements from 47 cities (Wang et al., 2013), and the online measurements from the Changdao site in Shandong Province (Yuan et al., 2013), with linear regression slopes in the range of 0.91–1.03. In addition, the summertime emission ratios for most NMHC species at the PKU site agreed with the results from 28 cities in the USA within a factor of two, with the exception of *i*-butane and 1-butene. Compared with results for London, UK (McMeeking et al., 2012), higher emission ratios of reactive alkenes and aromatics were found at the PKU site. Meanwhile, the emission ratios of most alkane species at the PKU site tended to be lower than results obtained in the Los Angeles and New England areas of the USA (Warneke et al., 2007), or those obtained in Mexico City (Bon et al., 2011). For OVOC species, the emission ratios of acetone and MEK at the PKU site were similar with the results in the New England area, but higher than those in Mexico City; conversely, methanol emission ratios were higher in PKU than those in either New England or Mexico City.

3.3.5 Estimation of VOC emissions in Beijing

On the basis of the emission ratios derived from measurements in Sect. 3.3.2, and the known CO emissions, the emission strengths of individual VOC species can be

calculated using the following equation:

$$E_{\mathrm{VOC,\,A}} = \left(\mathrm{ER}_{\mathrm{VOC,\,S}} \times E_{\mathrm{CO,\,S}} + \mathrm{ER}_{\mathrm{VOC,W}} \times E_{\mathrm{CO,\,W}}\right) \times \mathrm{MW}_{\mathrm{VOC}}/\mathrm{MW}_{\mathrm{CO}} \quad (6)$$

where $E_{\mathrm{VOC,\,A}}$ ($\mathrm{Gg\,yr^{-1}}$) is the annual emission of a particular VOC species; $\mathrm{ER}_{\mathrm{VOC,\,S}}$ and $\mathrm{ER}_{\mathrm{VOC,\,W}}$ are the emission ratios of VOCs to CO in the summer and winter, respectively; $\mathrm{MW}_{\mathrm{VOC}}$ and $\mathrm{MW}_{\mathrm{CO}}$ are the molecular weights of VOC and CO, respectively; and $E_{\mathrm{CO,\,S}}$ and $E_{\mathrm{CO,\,W}}$ are the emission strengths of CO during the summer (non-heating season, April–October) and winter (heating season, November–March), respectively. The magnitude of CO emissions is actually the most important factor affecting the accuracy of the calculation of VOC emissions using Eq. (6). Several studies have found that there are large uncertainties in CO bottom-up emissions inventories (Streets et al., 2006; Carmichael et al., 2003). Therefore, in order to calculate VOC emissions, we used CO emission data from Tang et al. (2013), which were obtained by the inverse modeling of online CO observations at 25 sites in Beijing. The values of $E_{\mathrm{CO,\,S}}$ and $E_{\mathrm{CO,\,W}}$ were estimated at 2392 and 2280 Gg, respectively, according to the inverse model results and the monthly variation in CO emission strength from Zhang et al. (2009). Annual anthropogenic emissions for individual VOC species estimated using this method are listed in Table S2.

The calculated annual emission strengths for individual VOC species were compared with the TRACE-P (Streets et al., 2003) and INTEX-B (Zhang et al., 2009) bottom-up inventories (Fig. 9a and b, respectively). The annual emission strengths for most NMHC species from the TRACE-P inventory were within a factor of two from the values calculated using Eq. (6); whereas, the emission strengths of benzene, ketones, and aldehydes were underestimated by $\geq 50\,\%$ in the TRACE-P inventory. The OVOC species emission strengths in INTEX-B inventory were also lower by a factor of ≥ 2 compared with the values derived from measurements. The underestimation trend for OVOC species in the bottom-up emission inventories may be caused by the following: (1) some OVOC sources were neglected or underestimated in bottom-up inventories; or (2) the emission factors for OVOC species from some sources were under-

estimated. There is some support for each of these possibilities in the literature. De Gouw et al. (2005) and Warneke et al. (2007) suggested that the primary sources of OVOC species in urban areas were not yet well understood, but that they were unlikely to be automobile emissions. This is consistent with the first hypothesis. Meanwhile, Zavala et al. (2009) compared the VOC emission factors derived from on-road measurements and those applied to calculate the gasoline vehicle inventory in Mexico City. They found that the emission factors for formaldehyde and acetaldehyde seemed to be underestimated by factors of three and two, respectively. This provides evidence for the second hypothesis. In addition, there are strong discrepancies for some NMHC species, with the INTEX-B inventory underestimating the emission strength of C2–C4 alkanes but overestimating both 1,3-butadiene and styrene emissions. Previous studies have found that C2–C4 alkanes can be emitted from the usage of natural gas (NG), liquefied petroleum gas (LPG) (Blake and Rowland, 1995) and gasoline. The lower emissions of C2–C4 alkanes in the INTEX-B inventory indicate that VOC emissions from NG, LPG and gasoline usage might be underestimated. Industrial sources were the most important contributor to 1,3-butadiene and styrene emissions in the INTEX-B inventory, with relative contributions of 70 % and 100 %, respectively. Therefore, the comparison results suggest that the INTEX-B inventory might overestimate the contribution of industrial emissions.

Several studies have used field measurement data for O_3 (Tang et al., 2011) and satellite data for glyoxal (Liu et al., 2012a) as constrains to validate VOC emission strengths in Beijing. Tang et al. (2011) suggested that emission strengths of total VOC might be overestimated in INTEX-B inventory, whereas Liu et al. (2012a) found aromatics might be underestimated in this inventory. However, the total emission for measured VOC species (see in Table S2) was estimated to be $419 \pm 201\,\mathrm{Gg\,yr^{-1}}$ in our study, slightly higher than the emission provided by INTEX-B inventory ($313\,\mathrm{Gg\,yr^{-1}}$). In addition, the calculated annual emissions for toluene and xylenes in our study agreed relatively well with values from INTEX-B inventory, with the relative difference of $\sim 20\,\%$. These findings are inconsistent with results from previous studies (Tang et al., 2011;

Liu et al., 2012a). One explanation for this inconsistence is that these studies used the measurement of secondary pollutants as constrain, and therefore they actually validated the capacity of VOC species to produce O_3 or glyoxal rather than VOC emission. Since the formation of these secondary pollutants is not only influence by VOC emission but also reaction mechanism or efficiency, it would be better to evaluate and validate VOC emission based on VOC measurement.

To further investigate the discrepancies between VOC emissions derived from measurements and existing emission inventories, and their effect on ozone production modeling, the total OH reactivity (s^{-1}) of all measured VOC species was calculated using the following equation:

$$\text{total OH reactivity} = \sum \text{OH reactivity}_{\text{VOC}} = \sum (\text{ER}_{\text{VOC}} \times k_{\text{VOC}} \times [\text{CO}]) \quad (7)$$

where k_{VOC} and ER_{VOC} are the OH rate constant and emission ratio of a particular VOC, respectively, and [CO] is the ambient mixing ratio of CO, which is assumed to be 1.0 ppmv. Figure 10 compares the total OH reactivity derived from measurements in this study and those calculated from the INTEX-B (Zhang et al., 2009) and TRACE-P (Streets et al., 2003) emission inventories. The results show that the total OH reactivity from these three studies was comparable, with values in the range of 8.4–9.3 s^{-1}. However, the relative contributions of different VOC groups to the total OH reactivity showed significant differences among these studies. Compared with results from measurements, the relative contributions of OVOC were lower in the bottom-up emission inventories, whereas alkene contributions were larger. This implies that if we were to use these two emission inventories as the input to a chemical transport model to predict ozone production in Beijing, the model may predict ambient ozone levels well, but could underestimate the OVOC contribution to ozone production, while overestimating the contribution of alkenes.

It should be noted that the "top-down" approach based on measurements has several limitations and uncertainties. First, in this case we used measurements carried out during August–September and December–January to derive VOC emission ratios during

non-heating and heating seasons, respectively. However, this still limits the temporal representation relative to continuous observations lasting more than one year. The difference in timing between the emission inventories (2000 for TRACE-P inventory, 2006 for INTEX-B inventory) and observations (2009–2012) is also a limitation. Another important source of uncertainty is the use of the CO inventory, which was the basis of calculating anthropogenic VOCs emissions. Even though the CO emission data applied in this study were calculated using the inverse modeling method (Tang et al., 2013), the CO measurements were only conducted during two weeks in July 2010, and therefore using these data to derive an annual CO emission dataset will increase the uncertainty of results.

3.4 VOC source apportionment

Source apportionment was performed using the CMB model to investigate the spatial and temporal variation characteristics of NMHC sources in Beijing. The calculated contributions were for eight main sources: gasoline vehicle exhaust (Exhaust_G), diesel vehicle exhaust (Exhaust_D), coal combustion, gasoline evaporation (Gasoline), LPG usage (LPG), paint and solvent usage (Paint & Solvent), biogenic sources, and the chemical industry (Industry). The CMB model performance parameters were within acceptable intervals, i.e., R^2 fluctuated between 0.65 and 0.98, and χ^2 ranged from 2.04 to 6.01. The percent mass concentrations explained by these eight sources varied between 81 % and 118 %.

3.4.1 Seasonal variation in NMHC sources

Figure 11a and b shows the average relative contributions of NMHC sources during summer and winter at the PKU site, respectively. In both seasons, gasoline vehicular exhaust was the largest source contributing to measured total NMHC mixing ratios, with an average relative contribution of ~ 50 %. During summer, the second largest contribution was from LPG usage (21 %), followed by gasoline evaporation (8 %), paint

and solvent usage (7 %), chemical industry (5 %), coal combustion (4 %), diesel exhaust (3 %), and biogenic emissions (1 %). Compared with NMHC sources in summer, the relative contribution of coal combustion increased to 19 % in winter, whereas the contributions from LPG usage, gasoline evaporation, paint and solvent usage, and biogenic emission decreased to 16 %, 3 %, 4 %, and 0.08 %, respectively. This significant seasonal difference in NMHC sources at the PKU site could be explained by the following reasons: (1) more coal was burned in winter for heating; (2) the high ambient temperatures in summer promote the evaporation of LPG, gasoline, and solvent emissions into atmosphere; and (3) biogenic emissions are favored by high light intensity and high ambient temperatures during the summer.

The NMHCs source apportionment results from regional measurement data showed similar seasonal variation characteristics with those at the PKU site. Vehicular exhaust (i.e., the sum of Exhaust_G and Exhaust_D) was the predominant NMHC source in Beijing, with relative contributions in the range of 41–53 %, but it did not show a clear seasonal variation pattern. Biogenic emissions and gasoline vaporization exhibited maximum contributions during the summer (May–August), with values of 3–4 % and 8–9 %, respectively (Fig. 12a). The relative contributions of LPG and paint and solvent usage also showed higher values in the summer compared to those in the winter. In contrast, chemical industry and coal combustion exhibited higher contributions in the winter (Fig. 12b). Possible explanations for the seasonal variation patterns in different NMHC sources have been discussed based on receptor model results at the PKU site, except for the petrochemical industry source. The largest petrochemical industry (Beijing Yanshan Petrochemical) is located in the southwest of Beijing (site I in Fig. 1). During the winter, the prevailing wind direction in Beijing is from the northwest or west, and thus this petrochemical industry could affect the NMHC measurement data obtained at those sites in southern areas of Beijing. However, the influence of this petrochemical industry would be lower during summer due to the south and southeast prevailing winds and the lower wind speeds.

3.4.2 Spatial variation in source contributions

Figure 11c shows the average relative contribution of NMHC sources based on all observations conducted at 27 sites from July 2009 to January 2011. Compared with the NMHC source structure at the PKU site, the relative contributions of industrial emission, diesel exhaust, and biogenic emissions were larger, with values of 17 %, 6 %, and 2 %, respectively, whereas the average contribution from gasoline vehicular exhaust decreased to 39 %.

To further investigate the spatial distribution of NMHC sources, the relative contributions of each source at the 27 sites were plotted on a map of Beijing. Figure 13a–d presents the annual average relative contributions of gasoline vehicular exhaust, diesel vehicular exhaust, chemical industry, and biogenic emissions at different sites in Beijing, respectively. Gasoline vehicular exhaust displayed the highest relative contribution in the downtown area (> 50 %) and the lowest contribution at the suburban or rural sites (< 25 %). The high density of gasoline vehicles in central Beijing may explain this finding. In contrast to the spatial distribution of gasoline vehicular exhaust, diesel vehicular exhaust exhibited higher contributions (> 10 %) in suburban and rural areas than in urban areas. This spatial distribution was likely associated with an increased use of diesel vehicles for agricultural activities in suburban and rural areas. Petrochemical industrial emissions showed the highest relative contributions (> 20 %) in the southern areas of Beijing, where industrial zones are located, such as the Beijing Development Area (the BOS1 site) and Beijing Yanshan Petrochemical site (the I site). For biogenic emissions, the largest contributions (> 4 %) were found in suburban and rural areas with higher vegetative cover. The relative contributions from the other three sources of gasoline vaporization, paint and solvent usage, and LPG usage did not show clear spatial distribution characteristics.

3.4.3 Comparison with bottom-up emission inventories

Table 1 compares the relative contribution of anthropogenic sources for Beijing city obtained in this study using the CMB model and those values from the bottom-up emission inventories (Su et al., 2011; Zhang et al., 2009; Bo et al., 2008; Wei et al., 2008). Both the CMB result based on ambient measurement data and the emission inventories show that vehicular emissions are the most important NMVOC source in Beijing, with relative contributions of 40–51 %. However, the relative contribution of solvent and paint usage obtained from the CMB model (5 %) was significantly lower than values from emission inventories (14–32 %). Meanwhile, the contribution from industrial processes estimated using the CMB model (17 %) was higher than that from emission inventories (10–14 %). However, it should be pointed out that the industrial emissions in the INTEX-B emission inventory also included industrial solvent utilization (Zhang et al., 2009). Since residential solvent utilization was small compared with industrial solvent usage, the relative contribution of industrial emissions from Zhang et al. (2009) can be considered to correspond to the sum of contributions from industrial processes and solvent and paint utilization in other studies (Industry & Solvent). The relative contribution of "Industry & Solvent" sources from the CMB model was 22 %, similar to that reported by Bo et al. (2008) (24 %); however, it was significantly lower than that of other inventories (43–46 %). The sum of LPG usage and gasoline evaporization contributions from CMB model was 21 %, significantly larger than the sum of petroleum storage and transportation from the emission inventories (5–6 %). The relative contributions of fossil fuel combustion showed large discrepancies among these emission inventories, with values ranging from 3 % to 15 %. The coal combustion contribution obtained from the CMB model was 10 %, within the range of emission inventories. Owing to the colinearity of NMVOC profiles between bio-fuel, biomass burning, and coal combustion, the former source was not included in CMB source apportionment. In addition, it should be noted that open biomass burning processes were included in the emission inventory established by Bo et al. (2008), whereas only bio-fuel combustion was considered in

other inventories. Wei et al. (2008) and Zhang et al. (2009) estimated that bio-fuel combustion contributed 11 % and 7 % to anthropogenic NMVOCs emissions, significantly higher than values from the other two inventories (2–4 %).

4 Conclusions

Ambient VOCs and CO mixing ratios were measured in Beijing and its surrounding areas from July 2009 to January 2012. Seasonal variations in VOC levels were observed in Beijing, with higher anthropogenic NMHCs but lower carbonyl mixing ratios in winter. The spatial distributions of measured VOC mixing ratios revealed a hotspot in southern suburban areas of Beijing, while the highest VOC emission strengths in current emission inventories were located in urban areas. Most of the measured VOC species exhibited significant correlations with CO, and the emissions ratios of individual VOC species were calculated based on the photochemical aging of air masses. The anthropogenic emissions of VOCs were then estimated based on the derived emission ratios and CO emissions calculated using an inverse modeling approach. The OVOC emissions estimated from measurements were larger than those of existing inventories, whereas alkene emissions were higher in inventories. Vehicular exhaust was identified as the largest contributor to VOCs in Beijing using the CMB model, with a contribution of 46 %, which agreed well with the range of 40–51 % given by current inventories. However, the contribution of solvent and paint utilization from the CMB was only 5 %, significantly lower than the values of 14–32 % in inventories. In addition, the LPG contribution from the CMB model reached 15 %, whereas the importance of LPG usage to VOC emissions was not reported by emission inventories. Using VOC measurement data to evaluate and validate the existing emission inventories is helpful in improving the prediction accuracy of air quality models. Additionally, identifying the reasons for the discrepancies between VOC emissions from measurement and inventory will help researchers to find out how to reduce the uncertainty of VOCs inventories.

Supplementary material related to this article is available online at http://www.atmos-chem-phys-discuss.net/13/26933/2013/acpd-13-26933-2013-supplement.pdf.

Acknowledgements. This study was funded by the Natural Science Foundation for Outstanding Young Scholars (Grant No. 41125018) and by the Beijing Municipal Science & Technology Commission (Project No. D09040903670904).

References

Atkinson, R. and Arey, J.: Atmospheric degradation of volatile organic compounds, Chem. Rev., 103, 4605–4638, doi:10.1021/cr0206420, 2003.

Atkinson, R., Baulch, D. L., Cox, R. A., Crowley, J. N., Hampson, R. F., Hynes, R. G., Jenkin, M. E., Rossi, M. J., Troe, J., and IUPAC Subcommittee: Evaluated kinetic and photochemical data for atmospheric chemistry: Volume II – gas phase reactions of organic species, Atmos. Chem. Phys., 6, 3625–4055, doi:10.5194/acp-6-3625-2006, 2006.

Baker, A. K., Beyersdorf, A. J., Doezema, L. A., Katzenstein, A., Meinardi, S., Simpson, I. J., Blake, D. R., and Rowland, F. S.: Measurements of nonmethane hydrocarbons in 28 United States cities, Atmos. Environ., 42, 170–182, doi:10.1016/j.atmosenv.2007.09.007, 2008.

Bertman, S. B., Roberts, J. M., Parrish, D. D., Buhr, M. P., Goldan, P. D., Kuster, W. C., Fehsenfeld, F. C., Montzka, S. A., and Westberg, H.: Evolution of alkyl nitrates with air mass age, J. Geophys. Res.-Atmos., 100, 22805–22813, doi:10.1029/95jd02030, 1995.

Blake, D. R. and Rowland, F. S.: Urban leakage of liquefied petroleum gas and its impact on Mexico City air quality, Science, 269, 953–956, doi:10.1126/science.269.5226.953, 1995.

Bo, Y., Cai, H., and Xie, S. D.: Spatial and temporal variation of historical anthropogenic NMVOCs emission inventories in China, Atmos. Chem. Phys., 8, 7297–7316, doi:10.5194/acp-8-7297-2008, 2008.

Bon, D. M., Ulbrich, I. M., de Gouw, J. A., Warneke, C., Kuster, W. C., Alexander, M. L., Baker, A., Beyersdorf, A. J., Blake, D., Fall, R., Jimenez, J. L., Herndon, S. C., Huey, L. G., Knighton, W. B., Ortega, J., Springston, S., and Vargas, O.: Measurements of volatile organic compounds at a suburban ground site (T1) in Mexico City during the MILAGRO 2006

campaign: measurement comparison, emission ratios, and source attribution, Atmos. Chem. Phys., 11, 2399–2421, doi:10.5194/acp-11-2399-2011, 2011.

Carmichael, G. R., Tang, Y., Kurata, G., Uno, I., Streets, D., Woo, J. H., Huang, H., Yienger, J., Lefer, B., Shetter, R., Blake, D., Atlas, E., Fried, A., Apel, E., Eisele, F., Cantrell, C., Avery, M., Barrick, J., Sachse, G., Brune, W., Sandholm, S., Kondo, Y., Singh, H., Talbot, R., Bandy, A., Thorton, D., Clarke, A., and Heikes, B.: Regional-scale chemical transport modeling in support of the analysis of observations obtained during the TRACE-P experiment, J. Geophys. Res.-Atmos., 108, 8823, doi:10.1029/2002JD003117, 2003.

Chen, S. P., Liu, T. H., Chen, T. F., Yang, C. F. O., Wang, J. L., and Chang, J. S.: Diagnostic modeling of PAMS VOC observation, Environ. Sci. Technol., 44, 4635–4644, doi:10.1021/es903361r, 2010.

Coll, I., Rousseau, C., Barletta, B., Meinardi, S., and Blake, D. R.: Evaluation of an urban NMHC emission inventory by measurements and impact on CTM results, Atmos. Environ., 44, 3843–3855, doi:10.1016/j.atmosenv.2010.05.042, 2010.

de Gouw, J. A., Middlebrook, A. M., Warneke, C., Goldan, P. D., Kuster, W. C., Roberts, J. M., Fehsenfeld, F. C., Worsnop, D. R., Canagaratna, M. R., Pszenny, A. A. P., Keene, W. C., Marchewka, M., Bertman, S. B., and Bates, T. S.: Budget of organic carbon in a polluted atmosphere: results from the New England air quality study in 2002, J. Geophys. Res.-Atmos., 110, D16305, doi:10.1029/2004jd005623, 2005.

Fu, T. M., Jacob, D. J., Palmer, P. I., Chance, K., Wang, Y. X. X., Barletta, B., Blake, D. R., Stanton, J. C., and Pilling, M. J.: Space-based formaldehyde measurements as constraints on volatile organic compound emissions in east and south Asia and implications for ozone, J. Geophys. Res.-Atmos., 112, D06312, doi:10.1029/2006jd007853, 2007.

Fuentes, J. D., Wang, D., Neumann, H. H., Gillespie, T. J., DenHartog, G., and Dann, T. F.: Ambient biogenic hydrocarbons and isoprene emissions from a mixed deciduous forest, J. Atmos. Chem., 25, 67–95, doi:10.1007/BF00053286, 1996.

Fujita, E. M., Watson, J. G., Chow, J. C., and Magliano, K. L.: Receptor model and emissions inventory source apportionments of non-methane organic gases in California's San Joaquin valley and San Francisco bay area, Atmos. Environ., 29, 3019–3035, doi:10.1016/1352-2310(95)00122-f, 1995.

Heald, C. L., Jacob, D. J., Fiore, A. M., Emmons, L. K., Gille, J. C., Deeter, M. N., Warner, J., Edwards, D. P., Crawford, J. H., Hamlin, A. J., Sachse, G. W., Browell, E. V., Avery, M. A., Vay, S. A., Westberg, D. J., Blake, D. R., Singh, H. B., Sandholm, S. T., Talbot, R. W., and

Fuelberg, H. E.: Asian outflow and trans-Pacific transport of carbon monoxide and ozone pollution: an integrated satellite, aircraft, and model perspective, J. Geophys. Res.-Atmos., 108, 4804, doi:10.1029/2003jd003507, 2003.

Hsu, Y. K., VanCuren, T., Park, S., Jakober, C., Herner, J., FitzGibbon, M., Blake, D. R., and Parrish, D. D.: Methane emissions inventory verification in southern California, Atmos. Environ., 44, 1–7, doi:10.1016/j.atmosenv.2009.10.002, 2010.

Kwok, E. S. C. and Atkinson, R.: Estimation of hydroxyl radical reaction-rate constants for gas-phase organic-compounds using a structure-reactivity relationship-an update, Atmos. Environ., 29, 1685–1695, doi:10.1016/1352-2310(95)00069-b, 1995.

Klimont, Z., Streets, D. G., Gupta, S., Cofala, J., Fu, L. X., and Ichikawa, Y.: Anthropogenic emissions of non-methane volatile organic compounds in China, Atmos. Environ., 36, 1309–1322, doi:10.1016/s1352-2310(01)00529-5, 2002.

Liu, Y., Shao, M., Fu, L. L., Lu, S. H., Zeng, L. M., and Tang, D. G.: Source profiles of volatile organic compounds (VOCs) measured in China: Part 1, Atmos. Environ., 42, 6247–6260, doi:10.1016/j.atmosenv.2008.01.070, 2008a.

Liu, Ying, Shao, Min, Lu, Sihua, Chang, Chih-chung, Wang, Jia-Lin, and Chen, Gao: Volatile Organic Compound (VOC) measurements in the Pearl River Delta (PRD) region, China, Atmos. Chem. Phys., 8, 1531–1545, doi:10.5194/acp-8-1531-2008, 2008b.

Liu, Y., Shao, M., Kuster, W. C., Goldan, P. D., Li, X. H., Lu, S. H., and De Gouw, J. A.: Source identification of reactive hydrocarbons and oxygenated VOCs in the summertime in Beijing, Environ. Sci. Technol., 43, 75–81, doi:10.1021/es801716n, 2009.

Liu, Z., Wang, Y. H., Vrekoussis, M., Richter, A., Wittrock, F., Burrows, J. P., Shao, M., Chang, C. C., Liu, S. C., Wang, H. L., and Chen, C. H.: Exploring the missing source of glyoxal (CHOCHO) over China, Geophys. Res. Lett., 39, L10812, doi:10.1029/2012gl051645, 2012a.

Liu, Z., Wang, Y., Gu, D., Zhao, C., Huey, L. G., Stickel, R., Liao, J., Shao, M., Zhu, T., Zeng, L., Amoroso, A., Costabile, F., Chang, C.-C., and Liu, S.-C.: Summertime photochemistry during CAREBeijing-2007: RO_x budgets and O_3 formation, Atmos. Chem. Phys., 12, 7737–7752, doi:10.5194/acp-12-7737-2012, 2012b.

Lu, K. D., Hofzumahaus, A., Holland, F., Bohn, B., Brauers, T., Fuchs, H., Hu, M., Häseler, R., Kita, K., Kondo, Y., Li, X., Lou, S. R., Oebel, A., Shao, M., Zeng, L. M., Wahner, A., Zhu, T., Zhang, Y. H., and Rohrer, F.: Missing OH source in a suburban environment near Beijing:

observed and modelled OH and HO_2 concentrations in summer 2006, Atmos. Chem. Phys., 13, 1057–1080, doi:10.5194/acp-13-1057-2013, 2013.

McMeeking, G. R., Bart, M., Chazette, P., Haywood, J. M., Hopkins, J. R., McQuaid, J. B., Morgan, W. T., Raut, J.-C., Ryder, C. L., Savage, N., Turnbull, K., and Coe, H.: Airborne measurements of trace gases and aerosols over the London metropolitan region, Atmos. Chem. Phys., 12, 5163–5187, doi:10.5194/acp-12-5163-2012, 2012.

Niedojadlo, A., Becker, K. H., Kurtenbach, R., and Wiesen, P.: The contribution of traffic and solvent use to the total NMVOC emission in a German city derived from measurements and CMB modeling, Atmos. Environ., 41, 7108–7126, doi:10.1016/j.atmosenv.2007.04.056, 2007.

Ohara, T., Akimoto, H., Kurokawa, J., Horii, N., Yamaji, K., Yan, X., and Hayasaka, T.: An Asian emission inventory of anthropogenic emission sources for the period 1980–2020, Atmos. Chem. Phys., 7, 4419–4444, doi:10.5194/acp-7-4419-2007, 2007.

Parrish, D. D.: Critical evaluation of US on-road vehicle emission inventories, Atmos. Environ., 40, 2288–2300, doi:10.1016/j.atmosenv.2005.11.033, 2006.

Seinfeld, J. H. and Pandis, S. N.: Atmospheric Chememistry and Physics: from Air Pollution to Climate Change, 2nd Edn., Wiley-Interscience, 2006.

Shao, M., Lu, S. H., Liu, Y., Xie, X., Chang, C. C., Huang, S., and Chen, Z. M.: Volatile organic compounds measured in summer in Beijing and their role in ground-level ozone formation, J. Geophys. Res.-Atmos., 114, D00g06, doi:10.1029/2008jd010863, 2009.

Shao, M., Huang, D., Gu, D., Lu, S., Chang, C., and Wang, J.: Estimate of anthropogenic halocarbon emission based on measured ratio relative to CO in the Pearl River Delta region, China, Atmos. Chem. Phys., 11, 5011–5025, doi:10.5194/acp-11-5011-2011, 2011.

Song, Y., Shao, M., Liu, Y., Lu, S. H., Kuster, W., Goldan, P., and Xie, S. D.: Source apportionment of ambient volatile organic compounds in Beijing, Environ. Sci. Technol., 41, 4348–4353, doi:10.1021/es0625982, 2007.

Streets, D. G., Bond, T. C., Carmichael, G. R., Fernandes, S. D., Fu, Q., He, D., Klimont, Z., Nelson, S. M., Tsai, N. Y., Wang, M. Q., Woo, J. H., and Yarber, K. F.: An inventory of gaseous and primary aerosol emissions in Asia in the year 2000, J. Geophys. Res.-Atmos., 108, 8809, doi:10.1029/2002jd003093, 2003.

Streets, D. G., Zhang, Q., Wang, L. T., He, K. B., Hao, J. M., Wu, Y., Tang, Y. H., and Carmichael, G. R.: Revisiting China's CO emissions after the Transport and Chemical Evolu-

tion over the Pacific (TRACE-P) mission: synthesis of inventories, atmospheric modeling, and observations, J. Geophys. Res.-Atmos., 111, D14306, doi:10.1029/2006jd007118, 2006.

Su, J., Shao, M., Lu, S., and Xie, Y.: Non-methane volatile organic compound emission inventories in Beijing during Olympic Games 2008, Atmos. Environ., 45, 7046–7052, doi:10.1016/j.atmosenv.2011.09.067, 2011.

Takegawa, N., Miyakawa, T., Kuwata, M., Kondo, Y., Zhao, Y., Han, S., Kita, K., Miyazaki, Y., Deng, Z., Xiao, R., Hu, M., van Pinxteren, D., Herrmann, H., Hofzumahaus, A., Holland, F., Wahner, A., Blake, D. R., Sugimoto, N., and Zhu, T.: Variability of submicron aerosol observed at a rural site in Beijing in the summer of 2006, J. Geophys. Res.-Atmos., 114, D00G05, doi:10.1029/2008jd010857, 2009.

Tang, X., Wang, Z. F., Zhu, J., Gbaguidi, A. E., Wu, Q. Z., Li, J., and Zhu, T.: Sensitivity of ozone to precursor emissions in urban Beijing with a Monte Carlo scheme, Atmos. Environ., 44, 3833–3842, doi:10.1016/j.atmosenv.2010.06.026, 2010.

Tang, X., Zhu, J., Wang, Z. F., and Gbaguidi, A.: Improvement of ozone forecast over Beijing based on ensemble Kalman filter with simultaneous adjustment of initial conditions and emissions, Atmos. Chem. Phys., 11, 12901–12916, doi:10.5194/acp-11-12901-2011, 2011.

Tang, X., Zhu, J., Wang, Z. F., Wang, M., Gbaguidi, A., Li, J., and Shao, M.: Inversion of CO emissions over Beijing and its surrounding areas with ensemble Kalman filter, Atmos. Environ., doi:10.1016/j.atmosenv.2013.08.051, in press, 2013.

von Schneidemesser, E., Monks, P. S., and Plass-Duelmer, C.: Global comparison of VOC and CO observations in urban areas, Atmos. Environ., 44, 5053–5064, doi:10.1016/j.atmosenv.2010.09.010, 2010.

Wang, B., Shao, M., Lu, S. H., Yuan, B., Zhao, Y., Wang, M., Zhang, S. Q., and Wu, D.: Variation of ambient non-methane hydrocarbons in Beijing city in summer 2008, Atmos. Chem. Phys., 10, 5911–5923, doi:10.5194/acp-10-5911-2010, 2010.

Wang, M., Shao, M., Chen, W. T., Lu, S. H., Wang, C., Huang, D. K., Yuan, B., Zeng, L. M., and Zhao, Y.: Measurements of C1–C4 alkyl nitrates and their relationships with carbonyl compounds and O_3 in Chinese cities, Atmos. Environ., 81, 389–398, doi:10.1016/j.atmosenv.2013.08.065, 2013.

Wang, X. S., Li, J. L., Zhang, Y. H., Xie, S. D., and Tang, X. Y.: Ozone source attribution during a severe photochemical smog episode in Beijing, China, Sci. China. Ser. B, 52, 1270–1280, doi:10.1007/s11426-009-0137-5, 2009.

Warneke, C., McKeen, S. A., de Gouw, J. A., Goldan, P. D., Kuster, W. C., Holloway, J. S., Williams, E. J., Lerner, B. M., Parrish, D. D., Trainer, M., Fehsenfeld, F. C., Kato, S., Atlas, E. L., Baker, A., and Blake, D. R.: Determination of urban volatile organic compound emission ratios and comparison with an emissions database, J. Geophys. Res.-Atmos., 112, D10S47, doi:10.1029/2006JD007930, 2007.

Wei, W., Wang, S., Chatani, S., Klimont, Z., Cofala, J., and Hao, J.: Emission and speciation of non-methane volatile organic compounds from anthropogenic sources in China, Atmos. Environ., 42, 4976–4988, doi:10.1016/j.atmosenv.2008.02.044, 2008.

Wu, L. L., Zeng, L. M., Yu, X. N., and Shao, M.: Determination of atmospheric CO and CH_4 by GC-FID equipped with a low-pressure injector, Acta Sci. Circumstantiae, 30, 1766–1771, 2010 (in Chinese).

Yao, B., Vollmer, M. K., Zhou, L. X., Henne, S., Reimann, S., Li, P. C., Wenger, A., and Hill, M.: In-situ measurements of atmospheric hydrofluorocarbons (HFCs) and perfluorocarbons (PFCs) at the Shangdianzi regional background station, China, Atmos. Chem. Phys., 12, 10181–10193, doi:10.5194/acp-12-10181-2012, 2012.

Yuan, B., Shao, M., Lu, S. H., and Wang, B.: Source profiles of volatile organic compounds associated with solvent use in Beijing, China, Atmos. Environ., 44, 1919–1926, doi:10.1016/j.atmosenv.2010.02.014, 2010.

Yuan, B., Shao, M., de Gouw, J., Parrish, D. D., Lu, S., Wang, M., Zeng, L., Zhang, Q., Song, Y., Zhang, J., and Hu, M.: Volatile organic compounds (VOCs) in urban air: how chemistry affects the interpretation of positive matrix factorization (PMF) analysis, J. Geophys. Res.-Atmos., 117, D24302, doi:10.1029/2012JD018236, 2012.

Yuan, B., Hu, W. W., Shao, M., Wang, M., Chen, W. T., Lu, S. H., Zeng, L. M., and Hu, M.: VOC emissions, evolutions and contributions to SOA formation at a receptor site in eastern China, Atmos. Chem. Phys., 13, 8815–8832, doi:10.5194/acp-13-8815-2013, 2013.

Zavala, M., Herndon, S. C., Wood, E. C., Onasch, T. B., Knighton, W. B., Marr, L. C., Kolb, C. E., and Molina, L. T.: Evaluation of mobile emissions contributions to Mexico City's emissions inventory using on-road and cross-road emission measurements and ambient data, Atmos. Chem. Phys., 9, 6305–6317, doi:10.5194/acp-9-6305-2009, 2009.

Zhang, Q., Streets, D. G., Carmichael, G. R., He, K. B., Huo, H., Kannari, A., Klimont, Z., Park, I. S., Reddy, S., Fu, J. S., Chen, D., Duan, L., Lei, Y., Wang, L. T., and Yao, Z. L.: Asian emissions in 2006 for the NASA INTEX-B mission, Atmos. Chem. Phys., 9, 5131–5153, doi:10.5194/acp-9-5131-2009, 2009.

Zhao, B., Wang, P., Ma, J. Z., Zhu, S., Pozzer, A., and Li, W.: A high-resolution emission inventory of primary pollutants for the Huabei region, China, Atmos. Chem. Phys., 12, 481–501, doi:10.5194/acp-12-481-2012, 2012.

Table 1. Comparison of the relative contributions (%) of anthropogenic NMVOC sources for Beijing city in this study and in bottom-up emission inventories.

Sources	This study	Wei et al. (2008)	Bo et al. (2008)	Zhang et al. (2009)	Su et al. (2011)
	2009–2011	2005	2005	2006	2008
Transportation	46	40	51	42	41
Industrial processes	17	14	10	43[b]	14
Solvent and paint utilization	5	32	14		32
Petroleum storage and transport	6[a]	–	6	–	5
LPG usage	15	–	–	–	–
Fossil fuel combustion	10	3	15	8	6
Bio-fuel and/or biomass combustion	–	11	4[c]	7	2

[a] The relative contribution of petroleum storage and transport from the CMB results in this study correspond to the contribution of gasoline evaporization.
[b] The relative contribution of industrial emissions from Zhang et al. (2009) correspond to the sum of industrial processes and solvent and paint utilization contributions in other studies.
[c] Open biomass burning was also included in this emission inventory.

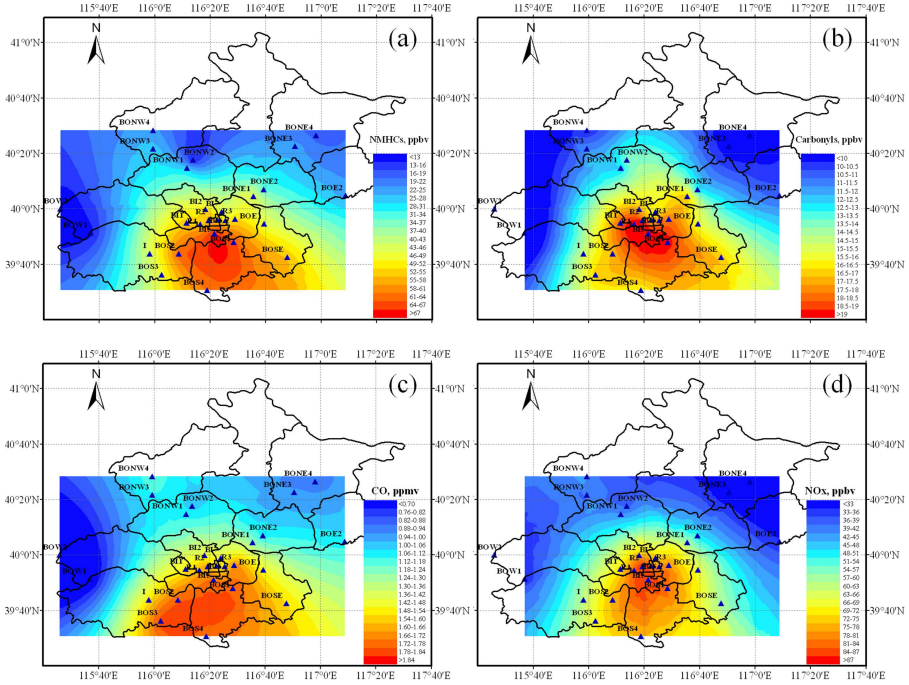

Fig. 1. Contour maps of annual average mixing ratios of **(a)** total NMHCs, **(b)** total carbonyls, **(c)** CO, and **(d)** NO_x in Beijing. Blue triangles indicate sampling locations and the names of these sites were listed in Table S1.

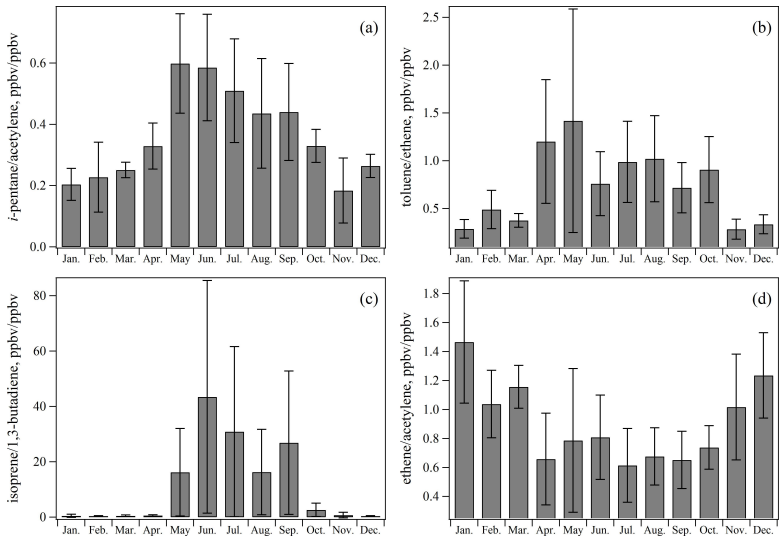

Fig. 2. Monthly variations in the average ratios of **(a)** *i*-pentane to acetylene, **(b)** toluene to ethene, **(c)** isoprene to 1,3-butadiene, and **(d)** ethene to acetylene at urban sites in Beijing. Error bars represent one standard deviation from the mean.

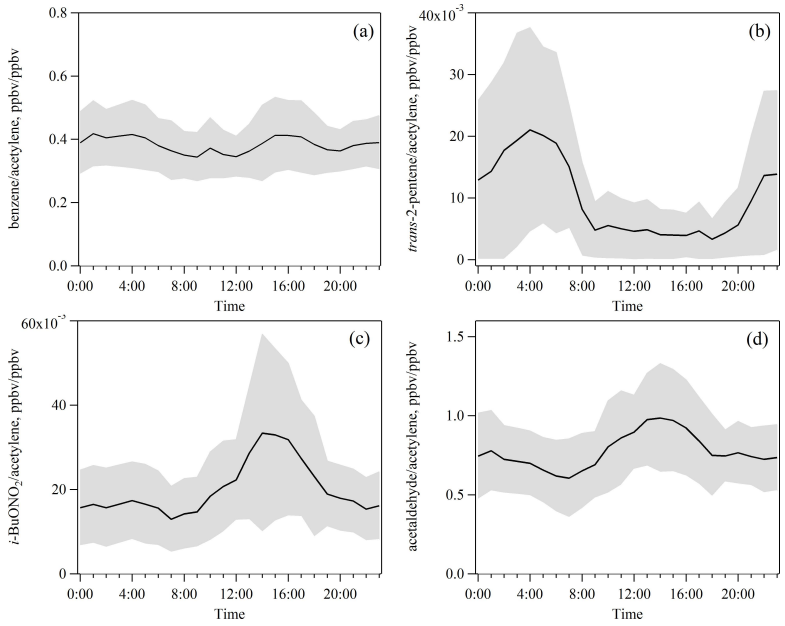

Fig. 3. Average diurnal variations in **(a)** benzene/acetylene, **(b)** *trans*-2-pentene/acetylene, **(c)** *i*-$BuONO_2$/acetylene, and **(d)** acetaldehyde/acetylene, measured during August 2011 at the PKU site. Grey areas represent one standard deviation from the hourly average ratio.

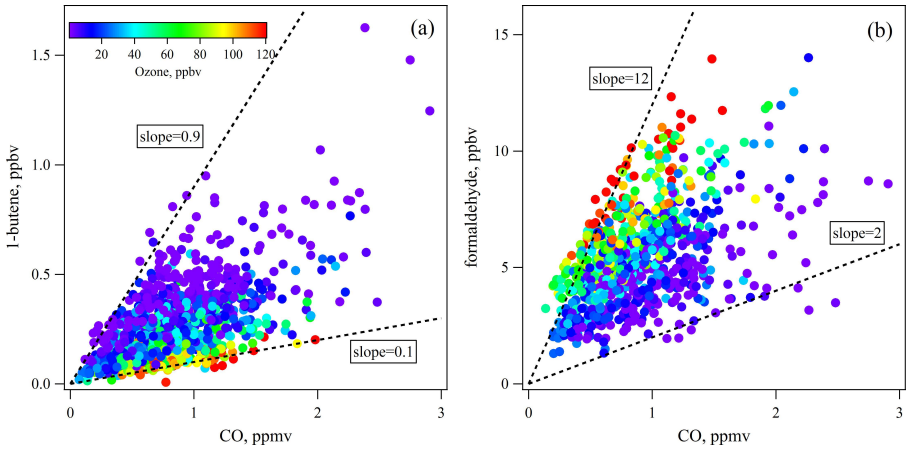

Fig. 4. Scatter plots of **(a)** 1-butene and **(b)** formaldehyde vs. CO measured at the PKU site during the summer in 2011. Data points are colored by O_3 levels.

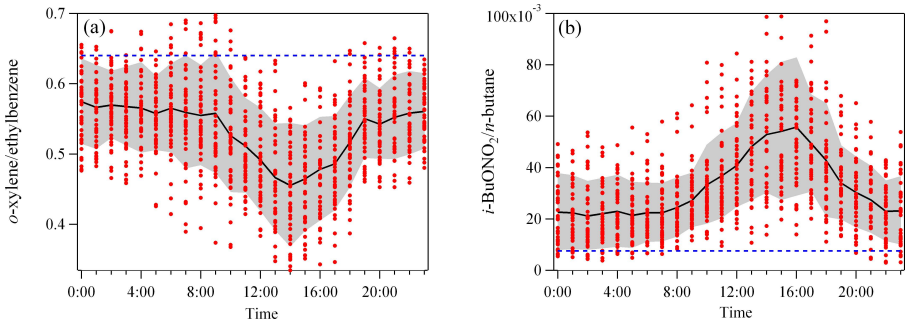

Fig. 5. Diurnal variation in hourly average ratios of **(a)** *o*-xylene/ethylbenzene (X/E), and **(b)** *i*-$BuONO_2$/*n*-butane. The red dots correspond to the measured ratios. The grey areas represent one standard deviation from the hourly average ratios. The blue dashed line corresponds to the average ratio at the time of emission.

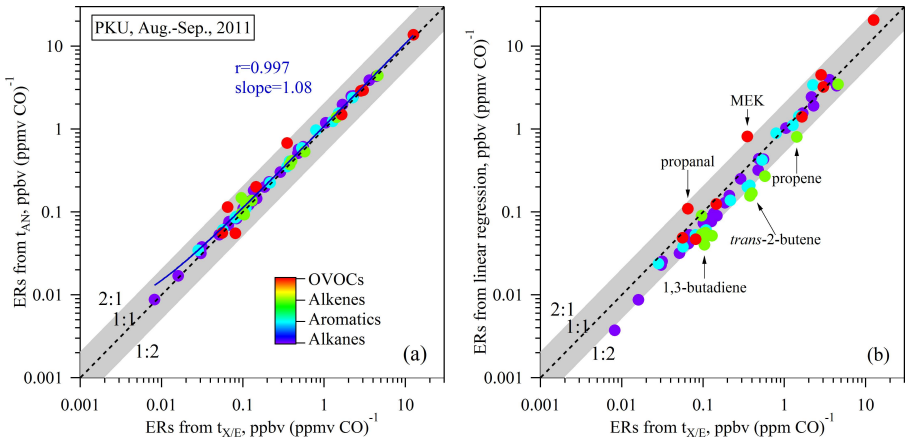

Fig. 6. Emission ratios of individual VOC species calculated based on photochemical ages derived from o-xylene/ethylbenzene ($t_{X/E}$) and compared with those obtained from **(a)** *i*-$BuONO_2$/*n*-butane (t_{AN}) or **(b)** ODR linear regression of nighttime measurement data. Each data point represents an individual VOC species, which is colored by VOC categories. The grey area represents the uncertainty range (±100 %). The black dashed lines and the blue line mean the 1 : 1 line and the best fit, respectively.

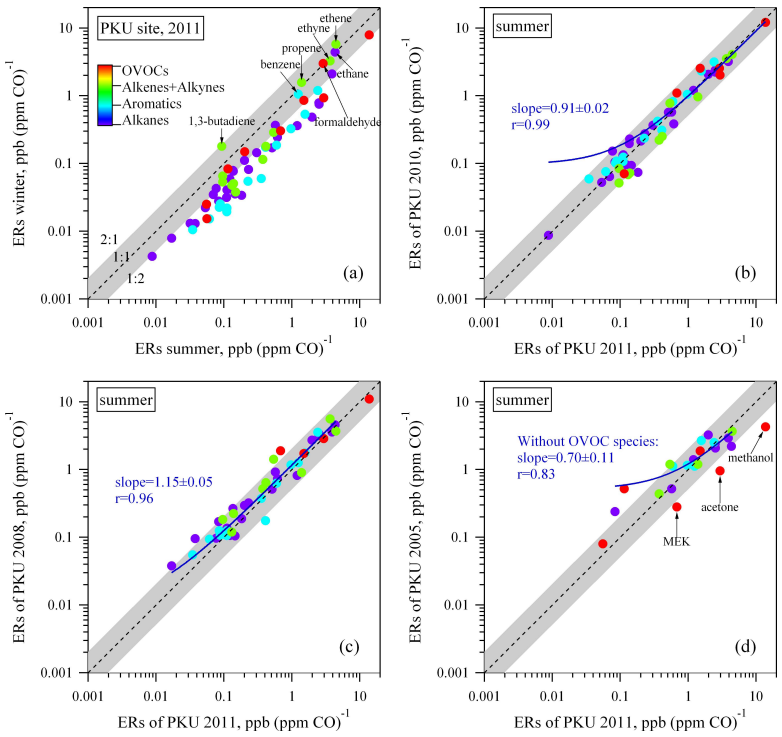

Fig. 7. Comparison of emission ratios of VOC species obtained at the PKU site: **(a)** winter vs. summer, **(b)** 2010 vs. 2011, **(c)** 2008 vs. 2011, and **(d)** 2005 vs. 2011.

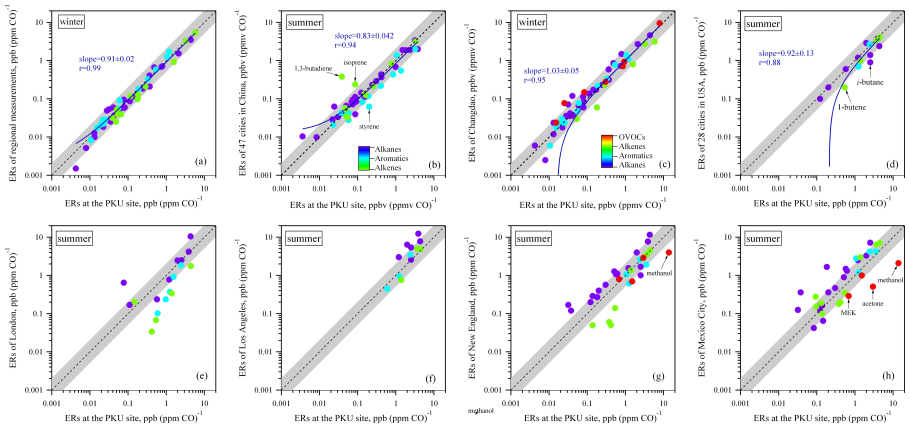

Fig. 8. Comparisons of the emission ratios of VOC species at the PKU site with values from **(a)** grided measurements in Beijing; **(b)** 47 cities in China (Wang et al., 2013); **(c)** the Changdao site in China (Yuan et al., 2013); **(d)** 28 cities in the USA (Baker et al., 2008); **(e)** London, UK (McMeeking et al., 2012); **(f)** Los Angeles, USA (Warneke et al., 2007); **(g)** New England area, USA (Warneke et al., 2007); and **(h)** Mexico City, Mexico (Bon et al., 2011).

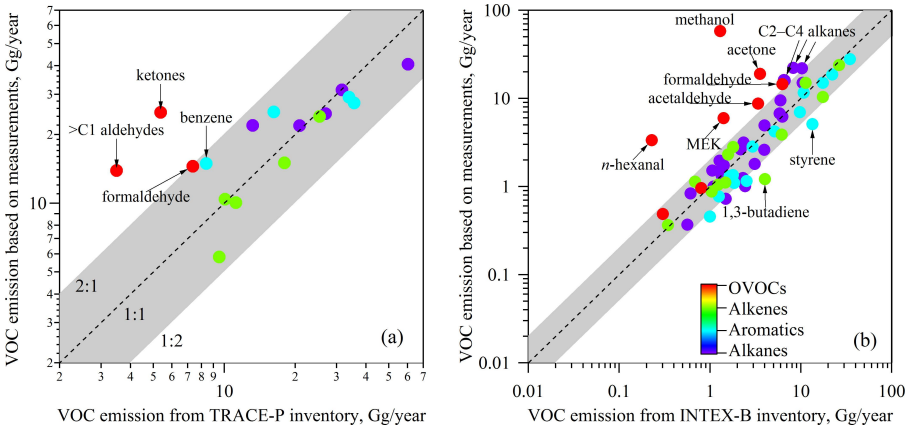

Fig. 9. Comparison of the annual emissions of VOC species estimated based on measurements in **(a)** TRACE-P (Streets et al., 2003) and **(b)** INTEX-B (Zhang et al., 2009) bottom-up emission inventories.

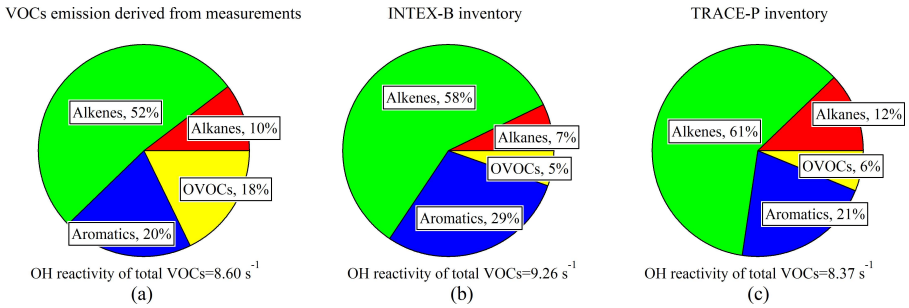

Fig. 10. Comparison of the relative contributions of VOC groups to the total OH reactivity of measured VOC species from **(a)** measurements, **(b)** the INTEX-B emission inventory (Zhang et al., 2009), and **(c)** the TRACE-P emission inventory (Streets et al., 2003). The OH reactivity for each VOC species was calculated as the product of its emission ratio, rate constant with OH (k_{OH}), and an assumed CO mixing ratio (1.0 ppmv).

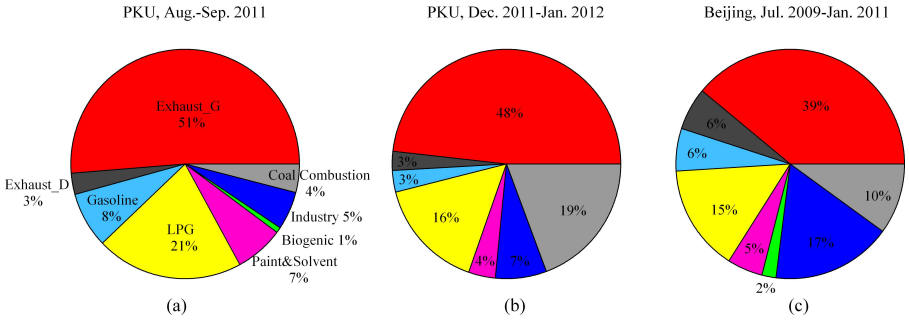

Fig. 11. Comparison of the average relative contributions of different sources to ambient NMHCs at the PKU site during **(a)** summer and **(b)** winter and **(c)** at 27 sites in Beijing from July 2009 to January 2011.

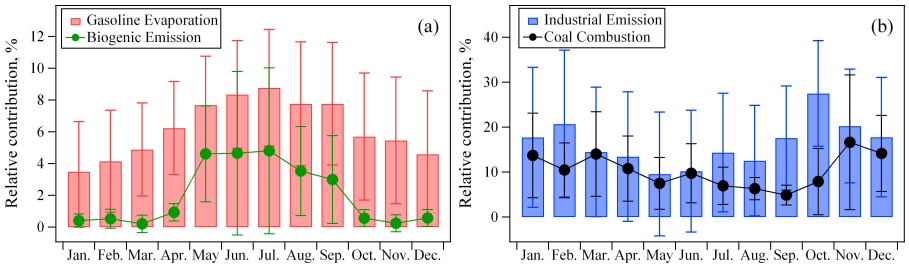

Fig. 12. Monthly variations in the average relative contributions of **(a)** gasoline evaporation and biogenic emissions, and **(b)** industrial emissions and coal combustion, at 27 sites of Beijing. The error bars reflect one standard deviation from the average relative contributions.

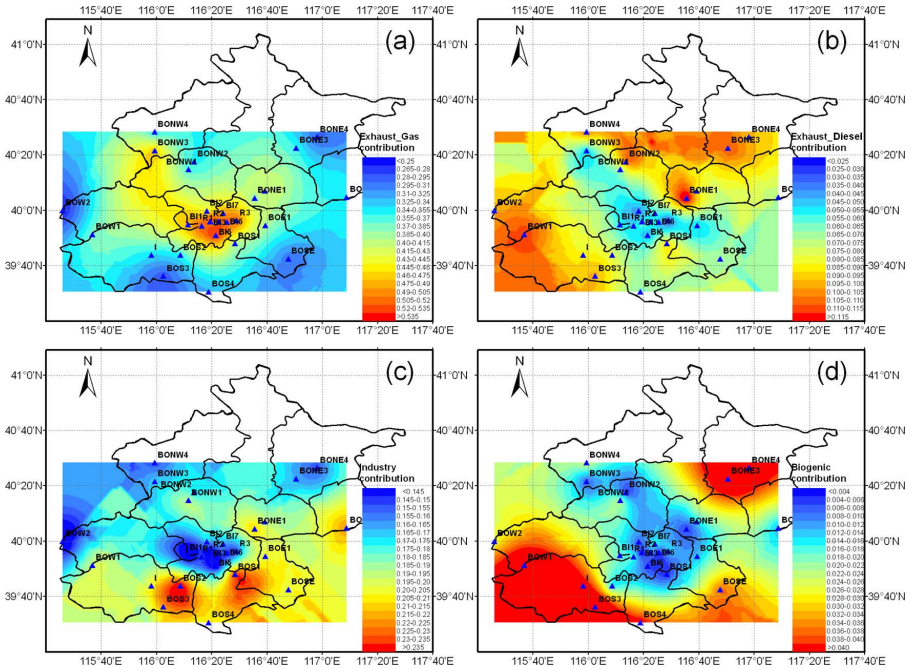

Fig. 13. Spatial distributions of the relative contributions of **(a)** gasoline vehicle exhaust (Exhaust_Gas), **(b)** diesel vehicle exhaust (Exhaust_Diesel), **(c)** chemical industry, and **(d)** biogenic emissions to ambient NMHC in Beijing.